

PROCEEDINGS OF SPIE

SPIEDigitalLibrary.org/conference-proceedings-of-spie

A review of earth abundant ZnO-based materials for thermoelectric and photovoltaic applications

Yang Wang, Chuanle Zhou, Aline M. Elquist, Amirhossein Ghods, Vishal G. Saravade, et al.

Yang Wang, Chuanle Zhou, Aline M. Elquist, Amirhossein Ghods, Vishal G. Saravade, Na Lu, Ian Ferguson, "A review of earth abundant ZnO-based materials for thermoelectric and photovoltaic applications," Proc. SPIE 10533, Oxide-based Materials and Devices IX, 105331R (23 February 2018); doi: 10.1117/12.2302467

SPIE.

Event: SPIE OPTO, 2018, San Francisco, California, United States

A review of earth abundant ZnO-based materials for thermoelectric and photovoltaic applications

Yang Wang^a, Chuanle Zhou^b, Aline M. Elquist^a, Amirhossein Ghods^b, Vishal G. Saravade^b, Na Lu^a, Ian Ferguson^b

^aLyles School of Civil Engineering, School of Materials Engineering, Birck Nanotechnology Center, Purdue University, West Lafayette, IN 47907, USA; ^bEngineering and Computing, Missouri University of Science and Technology, Rolla, MO 65409

ABSTRACT

Zinc oxide (ZnO) is an earth abundant wide bandgap semiconductor of great interest in the recent years. ZnO has many unique properties, such as non-toxic, large direct bandgap, high exciton binding energy, high transparency in visible and infrared spectrum, large Seebeck coefficient, high thermal stability, high electron diffusivity, high electron mobility, and availability of various nanostructures, making it a promising material for many applications. The growth techniques of ZnO is reviewed in this work, including sputtering, PLD, MOCVD and MBE techniques, focusing on the crystalline quality, electrical and optical properties. The problem with p-type doping ZnO is also discussed, and the method to improve p-type doping efficiency is reviewed. This paper also summarizes the current state of art of ZnO in thermoelectric and photovoltaic applications, including the key parameters, different device structures, and future development.

Keywords: ZnO, fabrication, p-type doping, thermoelectric, photovoltaic

1. INTRODUCTION

ZnO has drawn significant research attention for decades due to its earth abundancy, environmental friendly, and excellent structural, electrical, and optical properties. There are numerous applications of ZnO, such as ultraviolet (UV) light emitters¹, spin functional devices², gas sensors³, transparent electronics⁴ and acoustic wave devices⁵. In many respects, ZnO could be an excellent alternative to GaN for device applications due to its low production cost and better optical properties. However, repeatable and reliable p-type doping of ZnO remains an obstacle to producing a stable p-n junction of ZnO⁶. In this paper, growth and doping approaches of ZnO are reviewed. Recent progress in thermoelectric and photovoltaic applications of ZnO are discussed, and a review of fundamental issues for the realization of ZnO based devices is given.

1.1. Growth methods of ZnO films

Recent years have witnessed a revival and fast expansion in research on ZnO even though it is not a new semiconductor. It was initially used as a substrate for GaN growth due to the same wurtzite structure. The superior optical properties of ZnO, and the availability of high quality bulk material encouraged many research groups to turn their research on electronic and photonic devices of ZnO materials. Its high electron mobility, high thermal conductivity, wide direct band gap, and large exciton binding energy makes ZnO ideal for a variety of devices. These devices include transparent thin-film transistors, photodetectors, light-emitting diodes (LED) and laser diodes that operate in the blue and ultraviolet region of the spectrum. To facilitate these potential applications, research related to the growth of high quality ZnO thin films has boosted in recent years, including chemical vapor deposition (CVD), metalorganic chemical vapor deposition (MOCVD), atomic layer deposition (ALD), molecular beam epitaxy (MBE), pulsed laser deposition (PLD), plasma enhanced chemical vapor deposition (PECVD), sol-gel technique, and magnetron sputtering. Table 1 is a survey of typical growth methods of ZnO films. In the following, we briefly describe the results of ZnO thin films grown by sputtering, PLD, MOCVD and MBE techniques, focusing on the crystalline quality, electrical and optical properties.

Table 1 Growth methods, applications, growth substrates electrical and optical properties of ZnO layers

Method	Substrate	Resistivity (Ohm*cm)	Carrier Concentration (/cm ³)	Mobility (cm ² /V)	Refs.
Sputtering	Si	4.7*10 ⁻⁴	7.5*10 ²⁰	100	7
Sputtering		8*10 ⁻⁴	2.5*10 ²⁰	39	8
PLD	Sapphire		2*10 ¹⁸ -4*10 ¹⁹		10
PLD	Sapphire		10 ¹⁶ -10 ¹⁸	30-140	11
ALD	Glass	6.9*10 ⁻⁴	1.4*10 ¹⁹ -4.3*10 ¹⁹	23-33	12
MBE	Si	0.33	1.87*10 ¹⁸	10	14
MBE	Sapphire/ SiC		9*10 ¹⁸	260	15
MOCVD	Si				16
MOCVD	Sapphire				17

Magnetron Sputtering is a Plasma Vapor Deposition (PVD) process. The positive ions from the plasma are accelerated and strike the negative electrode to dislodge and eject atoms from the target. These atoms will be emitted in a typical line-of-sight cosine distribution from the face of the target and will condense on surfaces that are placed in proximity to the magnetron sputtering cathode. It is the most scalable technique and can generate films with great electrical properties. Carrier concentration in magnitude of 10²⁰ 18 and mobility of 100 cm²/V 8 are typically reported. It is challenging to grow defect free thin films with this method, because it is difficult to control the particles superimposed on the cathode.

Pulsed laser deposition uses a high-power laser beam strikes a target of known composition. A highly directional plume of gas material is produced and condensed onto a substrate. Targets used for growing ZnO films by PLD are sintered ceramic disks prepared from high-purity pressed powders. The powders are either ZnO single crystals, or pure Zn with a reactive oxygen atmosphere. Doped ZnO and alloys such as MgZnO and CdZnO can be achieved by including the alloying elements and dopants in the target or using a reactive gas in the chamber. Glass substrates as well as single-crystal substrates have been used to grow ZnO thin films using PLD, with the best results obtained using the latter. Sapphire is the most common substrate due to the large availability of single crystal wafers, low cost, and similar lattice. Other single-crystal substrates used to grow ZnO by PLD includes Si, GaAs, InP, CaF₂ and LiTaO₃, however, most of these substrates have a larger lattice mismatch with ZnO. Lattice mismatch causes the deposited films to develop large crystallites separated by grain boundaries. Grain boundaries can be detrimental to semiconductor applications. The relatively low Hall mobility, 30-140 cm²/V 11, observed in PLD ZnO films is attributed to the dominance of charge scattering at grain boundaries. Recent results of PLD ZnO films grown on ScAlMgO₄ (SCAM) deserve special attention. SCAM has a relatively small lattice mismatch of 0.09% with ZnO, and has proven to be the best alternative to sapphire substrates.

Metal organic chemical vapor deposition and molecular beam epitaxy are expected to produce better ZnO films in terms of crystalline quality at the expense of growth rates and with more complicated setups. In MOCVD the epitaxial layers grow via chemical reactions of the constituent chemical species at or near the heated substrate. In contrast, the epitaxial films in MBE are grown by physical deposition. MOCVD takes place in gas phase at moderate pressures, and has become the preferred technique for the growth of devices, and the dominant process for the manufacture of laser diodes, solar cells and LEDs. Promising results have already been obtained with MOCVD growth of ZnO films, with the best layers obtained

by homoepitaxy. MOCVD ZnO films have been grown on a wide range of substrates including glass, sapphire, Si, Ge, GaAs, GaP, InP, GaN and ZnO, with carrier concentrations varying from 10^{15} to 10^{20} cm^{-3} . Fewer studies have been performed using MBE growth of ZnO epitaxial layers, firstly reported in 1996. Substrates include sapphire, LiTaO₃, MgO and GaN. Carrier concentrations from 10^{16} to 10^{18} cm^{-3} , and mobilities ranging 90–260 $\text{cm}^2 \text{V}^{-1}\text{s}^{-1}$ have been reported¹⁵.

1.2. Challenge of commercializing ZnO: native defects

Although n-type ZnO is relatively easy to achieve, obtaining p-type ZnO has proven to be challenging, due to a high hole compensation by native point defects. Native point defects refer to lattice imperfections such as vacancies, interstitials and antisites. In ZnO particularly, there are two categories of native point defects, donor-like and acceptor-like defects. Donor-like defects include zinc interstitial atoms (Zn_i), oxygen vacancies (V_o), and zinc antisite atoms (Zn_o). Acceptor-like defects include oxygen interstitial atoms (O_i), zinc vacancies (V_{Zn}), and oxygen antisite atoms (O_{Zn}). Computational studies have shown that acceptor-like defects, such as V_o , have low formation energy and are predicted to form readily. In contrast, acceptor-like defects such as O_{Zn} have high formation energy, and therefore are difficult to form, and unstable at room temperature. Figure 1 shows the results of density functional theory (DFT) calculations on formation energies of native point defects in ZnO under Zn-rich and O-rich conditions. Figure 1 shows donor-like defects, Zn_i , V_o and Zn_o have much lower formation energy, thus they are much easier to form and thermodynamically more stable than acceptor-like defects. Lower formation energy of donor-like defects is responsible for the intrinsic n-type conductivity of un-doped ZnO. Generally, the mission to explore p-type doped ZnO requires suppressing donor-like defects and enhancing acceptor-like defects, as well as adding extrinsic acceptor dopants. A more detailed analysis on the physics of native defects can be found in other review paper^{19 20}.

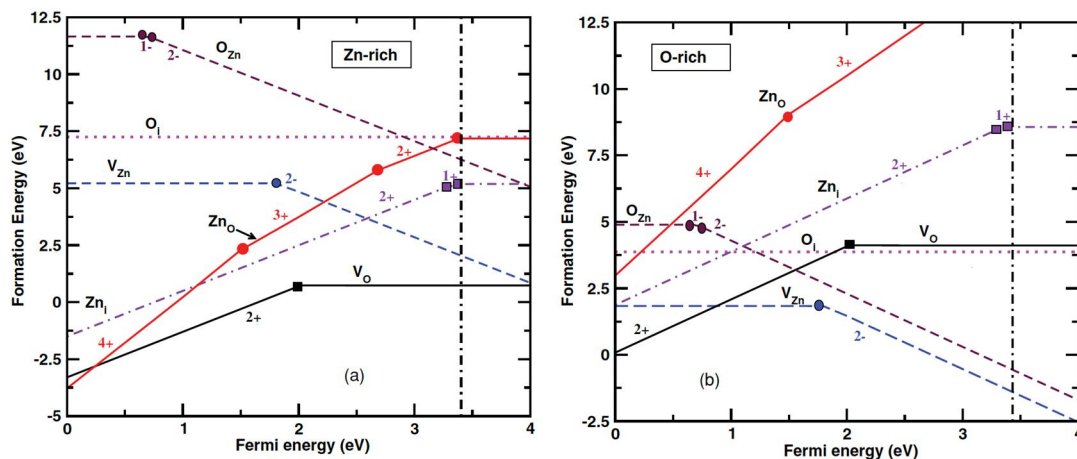


Figure 1. Formation energy of intrinsic defects in different charge states as a function of Fermi level²⁰

2. P-TYPE DOPED ZnO

The simplest and most straight forward way to achieve p-type conductivity ZnO is to dope it with group-I and group-V elements. Theoretical calculations based on density functional theory with local density approximation (LDA) or general gradient approximation (GGA)^{21,22}, predicted that substitutions of Zn with group-I or group-V elements act as shallow acceptors, which leads to p-type behavior. However, due to the limitations of density functional theory, the predictions of dopant energy levels were optimistic²³. Experimental results prove that measurable p-type conductivity is extremely difficult to achieve. The development of spin-polarized Kohn-Sham theory and hybrid functional has corrected dopant energy levels, and acceptor levels are shown to be much deeper than originally predicted. Despite the evidence that group-I and V elements are not desirable shallow acceptors, mono doping with group-I and V elements has been extensively studied, Table 2. An increasing number of groups have switched their interest from thin films to other nano structures such

as nano rods, nano particles, etc, due to easier availability of p-type conductivity in these other nanostructures than in films. As can be seen in table 2, for group-I and V dopants, relatively high resistivity and low hole mobility and concentration indicates high self-compensation and poor crystalline quality.

Table 2. Recent progress in p-type mono-doped ZnO thin film

Dopant	Method	Carrier Concentration (/cm ³)	Mobility (cm ² /V)	Resistivity (Ohm*cm)	Ref.
Ag	PLD	3*10 ¹⁶ –5*10 ¹⁷	0.3–1.5	43 – 136	24
Li	Solution	5.08*10 ¹⁹	0.01	11.62	25
Na	PLD	3.3*10 ¹⁷	0.28	67.43	28
K	Solution	3.7*10 ¹⁴ –3.8*10 ¹⁷			29
Al	Sputtering	2.5*10 ²⁰ –8*10 ²⁰	50–250	3*10 ⁻⁵ – 4*10 ⁻⁴	32
Al	Sputtering	6*10 ²¹	12	2.24*10 ⁻³	33
As	Sputtering	10 ²⁰	2.1		34
As	MOCVD	1.7*10 ¹⁹	36	0.01	36
N	MBE	1.96*10 ¹⁷ –1.68*10 ¹⁸	1.98–5.81	2.5–9.8	37
N	ALD	4.5*10 ¹⁶ –1.510 ¹⁷	1.73	6.9–8.0	40

P-type conductivity was observed group-I dopants: Ag, K, Li and Na with various techniques as shown in table 2. Due to the small size and high diffusivity of group-I elements, their use in mono doping has suffered from self-compensation. Instead of substituting Zn sites and serving as acceptors, group-I atoms tend to diffuse into interstitial sites and compensate holes. There are reports that Li in an as-grown sample can occupy interstitial sites of the ZnO wurtzite structure, and thermal annealing can assist the substitution of Zn with Li, however low hole concentration, low mobility, and high resistivity are still not improved. In recent years Al, Mg and Cd are considered promising candidates for p-type doping due to their lower diffusivity in ZnO. They tend to stay in Zn sites better than group-I elements, and serve as acceptors. Al results in high carrier concentration, high mobility, and low resistivity on the order of 10⁻⁵ Ohm*cm. Most Al doped ZnO films are fabricated by magnetron sputtering, so film quality is an issue for device fabrication. Growth of low defect and low resistivity Al doped ZnO with MOCVD or MBE could be an opportunity to integrate this material into devices.

For mono doping with group-V elements, N and Sb are two heavily investigated elements. As shown in table 2, they have relatively low resistivity and high carrier concentration. Researchers have found that N₂ and NO molecules at O sites are two complexes that will eliminating holes. A high concentration of N dopants is needed to suppress compensation before reliable p-type conductivity can be achieved. Sb atoms tend to occupy Zn sites due to their large atomic radius. When Sb occupies a Zn site, Sb_{Zn-2}V_{Zn} complex will be formed by combining Sb antisite and Zn vacancy near stacking faults. This only happens when Sb concentration is lower than 1%. At higher concentration Sb in an oxygen site, Sb_o, is more energetically favorable and could cause compensation of holes. To conclude, much improvement has not been reported in high performance p-type conductivity with mono doping. There have been device applications in which p-type conductivity is observed, showing the feasibility of p-type doping. It also gives a better idea which approach can lead to a reliable p-type dopant once we fully understand the underlying physics of each dopant.

Table 3. Recent progress in p-type co-doped ZnO thin film

Dopant	Method	Carrier concentration (/cm ³)	Mobility (cm ² /V)	Resistivity (Ohm*cm)	Ref.
B-N	MBE	1.3*10 ¹⁷ -3*10 ¹⁸	0.3-6.3	2-186	42
Al-N	Sputtering	5.84*10 ¹⁹ -8.3*10 ¹⁹	1.01-1.28	0.551-1.141	43
Al-P	Sputtering	3.7*10 ¹⁸	13.5	0.14	44
In-N	MOCVD	7.8*10 ¹⁷ -3.6*10 ¹⁸	0.11-0.5	15-16	45
Ag-N	Sputtering	3.07*10 ¹⁶	2.20	92.57	46
Li-N	PLD	1.55*10 ¹⁶ -7.56*10 ¹⁷	3.3-266.8	0.09-1.1	47
P-N	Sputtering	1.16*10 ¹⁸	1.35	3.98	48
Mg-Ag	PLD	2.85*10 ¹⁵ -7.89*10 ¹⁷	0.32-0.56	24.96-2812	49
Be-N	MBE	5.32*10 ¹⁶	0.33	N/A	50
Se-N	Sputtering	2.42*10 ¹⁵ -1.14*10 ¹⁶	0.151-0.238	2295-17120	51
Te-N	MOCVD	10 ¹⁷ -10 ¹⁸	1-10	1-10	52
Te-N	MOCVD	10 ¹⁶ -10 ¹⁷			53
Te-N	MBE	6*10 ¹⁵ -1.6*10 ¹⁶	1.8-16	18-210	54
S-P	Sputtering	10 ¹⁴ -10 ¹⁶	N/A	N/A	55

Since p-type conductivity with simple mono-doping approach is not that satisfactory and relatively unstable, various co-doping approaches have been experimentally implemented to enhance electrical conductivity and structural stability. Table 3 listed recent experimental progress in co-doped p-type ZnO thin film and corresponding electrical properties. As shown in the table, low resistivity and stable p-type doping in ZnO is far from being achieved. At this stage, there is no simple conclusion on which doping strategy is the best as there are many factors to be considered, such as acceptor energy level, formation of dopant complex, solubility, etc.

3. APPLICATIONS

3.1. TE application

Over the past decades, thermoelectric (TE) materials have drawn significant research attention. TE materials are used in power generation devices that can convert waste heat into electricity, refrigeration devices for cooling applications, and much more. The conversion of waste heat to useful energy could reduce the use of fossil based fuels. Reduced use of nonrenewable resources can reduce many environmental problems, such as air pollution, greenhouse effect, etc. To facilitate TE applications, researchers have discovered many materials that have good TE properties, such as Bi₂Te₃ and Sb₂Te₃, however they are expensive, toxic, and unstable at high temperatures. Oxide materials are earth abundant, and more stable in oxidizing environments. Although TE properties of oxides are inferior to those compounds mentioned above, its stability and low cost may enhance its potential for TE energy conversions.

Among potential TE oxide materials, ZnO presents a large Seebeck coefficient, high thermal stability, and it is non-toxic. Recent investigation on ZnO ceramics show their TE properties can be improved by doping with Al, Ti, Sb or Ni. Colder et al.⁵⁶ prepared Ni doped ZnO oxide ceramics using liquid rout and conventional sintering. The samples with x values below 0.03 show a dense microstructure of a single phase wurtzite ZnO structure, whereas the other samples present a secondary phase identified as cubic (Zn_xNi_xO). Figure 2 shows the power factor (PF) was optimized for $x = 0.03$, reaching a value of $0.56mWm^{-1} K^{-2}$ at 900 K. It also shows the doped element is effective in reducing the thermal conductivity at room temperature. The highest power factor ($0.6mWm^{-1}K^{-2}$) and ZT (0.09) were obtained in the composition $Zn_{0.97}Ni_{0.03}O$ (0.09 at 1000 K) as shown in figure 3.

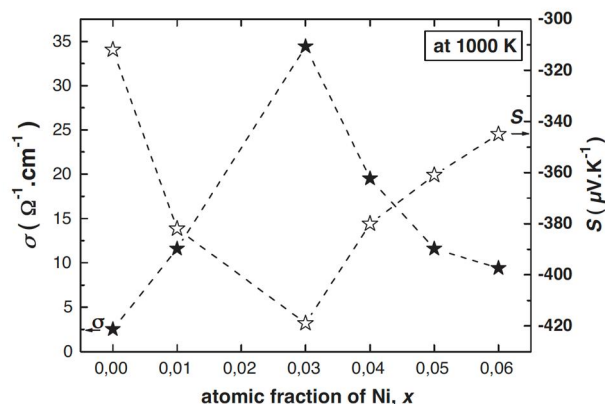


Figure 2. Electrical conductivity and Seebeck coefficient at 1000K versus atomic fraction of Ni, x⁵⁶

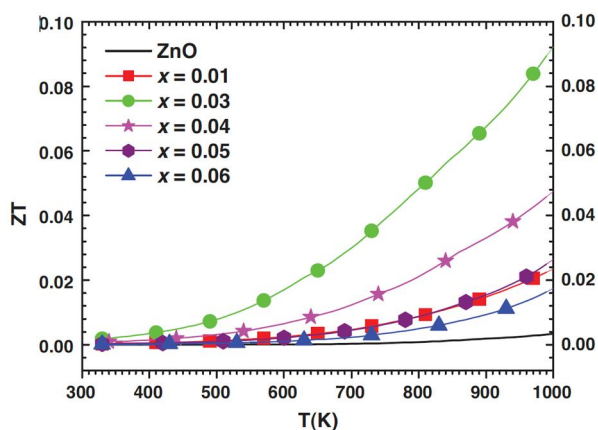


Figure 3. Temperature dependence of the figure of merit ZT of ZnO and Ni-doped ZnO⁵⁶

Another high power factor ZnO material was reported by Kwang-Hee Jung et al.⁵⁷ with Ga doped n-type ZnO. In this work, $Zn_{1-x}Ga_xO$ was prepared through solid-state synthesis using ZnO and Ga_2O_3 as starting materials. The powders were ball milled with ethanol and zirconia balls, then pressed by cold isotropic press at 200 MPa, followed by sintering at 1100 Celsius in N_2 . Figure 4 shows various Ga dopant concentrations conductivity, hall mobility, carrier concentration, Seebeck coefficient, thermal conductivity, and power factor as a function of temperature. Carrier concentration in magnitude of 10^{20} and hall mobility of $40-60 cm^2V^{-1}s^{-1}$ were observed, and above all, a power factor of $12.5 uWcm^{-1}K^{-2}$ and 0.25 ZT at 1000 Celsius were obtained, which is a huge advancement in TE performance for ZnO based TE materials.

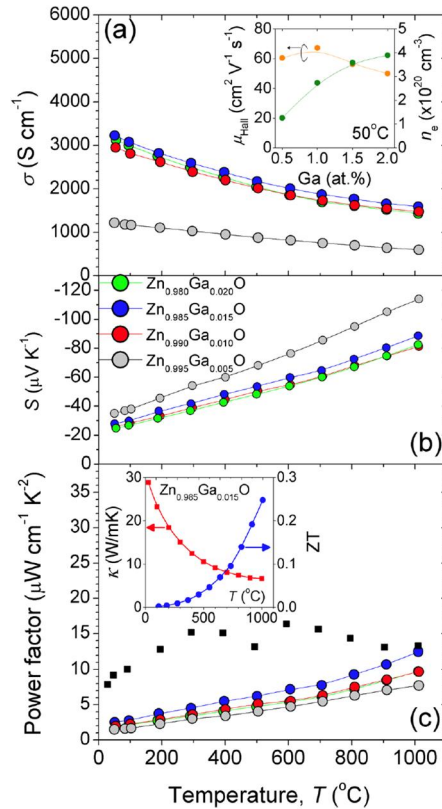


Figure 4. Temperature dependence of (a) electrical conductivity, hall mobility and carrier concentration (b) Seebeck coefficient and (c) power factor with various Ga concentrations ⁵⁷

High cost and complicated fabrication techniques still restrict the applications of thermoelectric generators (TEG). Ping Fan et al. ⁵⁸ demonstrated a flexible thin film TEG (TFTEG), the schematic of their TEG is shown in figure 5. By using DC sputtered Al-doped n-type ZnO and Sb-doped p-type ZnO films and flexible substrates, they greatly reduced the cost to produce TFTEG, about 4-5 times cheaper than Bi-Te-Se and Bi-Sb-Te TE materials. These results increased the potential for large-scale industrialization of TEGs. Figure 6 shows the electrical performance of the TFTEG as a function of temperature difference with room temperature cold side. The maximum output power for the 10-unit-generator reaches 246.3 μW when the temperature difference is 180K, which is several times that of other thin film TEGs reported.

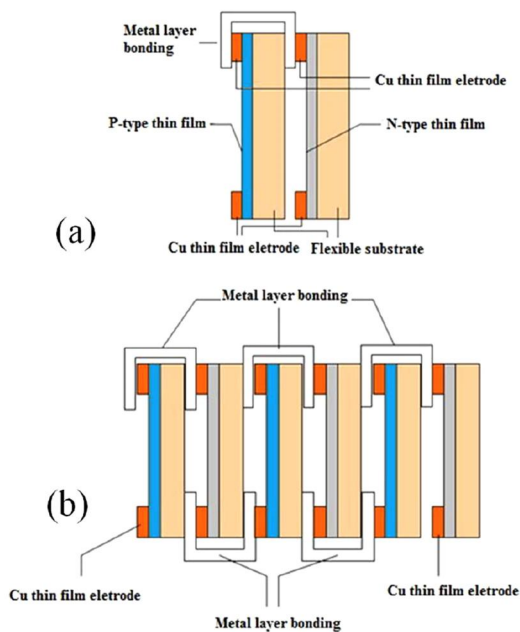


Figure 5. Schematic illustration of the TFTEG. (a) A p-n couple was formed through connecting the n- and p-type films by metal layer bonding with Cu films deposited on the both sides of the substrate. (b) Structure of the whole TFTEG.⁵⁸

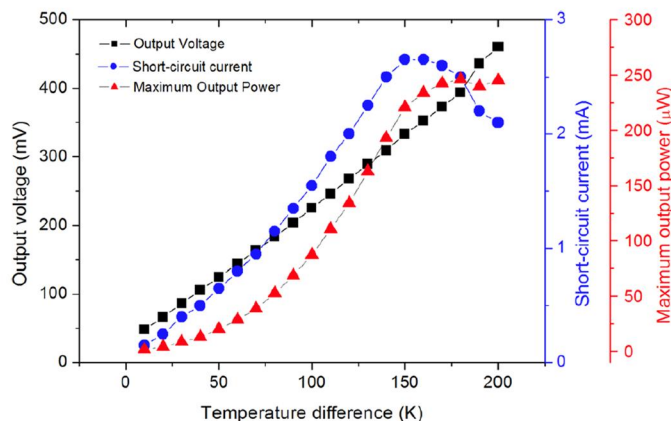


Figure 6. Electrical performance of TFTEG as function of temperature difference with fixed code side temperature of 300K.⁵⁸

3.2. ZnO for Photovoltaic Applications

ZnO has a wide direct bandgap, high electron diffusivity, high electron mobility and an energy-band structure favorable for electron transport with low solar spectrum absorption⁵⁹⁻⁶². ZnO also has the advantage of non-toxic and abundant earth presence, easy crystallization and anisotropic growth, which allows the fabrication of a wide variety of nanostructures, such as nanowires (NWs), nanorods (NRs), nanobelts, nanoparticles, hierarchical aggregates, porous films, nanosheets, and many other structures^{59,63-65}. ZnO-based nanostructures have been extensively studied as transparent electrodes⁶¹⁻⁶⁶, active layer⁶⁷⁻⁷⁴, and electron transport/hole blocking layer⁶²⁻⁶⁵, for dye-sensitized solar cells⁶²⁻⁶⁵, hybrid organic-inorganic solar cells⁷⁵, and polymer-based solar cells⁶⁰.

Transparent conducting oxides (TCO) ^{61,66,76} layers have been tremendously used in photovoltaic devices as transparent front contacts, diffusion barriers for carriers, and light trap in solar cells. The outstanding electrical conductivity and optical transparency of ZnO in the visible light spectrum (Figure. 7) ⁶⁶ makes it a good candidate TCO. Although ZnO thin films' resistivity is not as good as that of Sn-doped In₂O₃ (ITO), it offers benefits of low cost, and high chemical and thermal stability compared to In-based systems. ZnO TCOs can achieve impressive properties for different applications through substitutional doping with aluminum, indium, boron or gallium ⁶⁶.

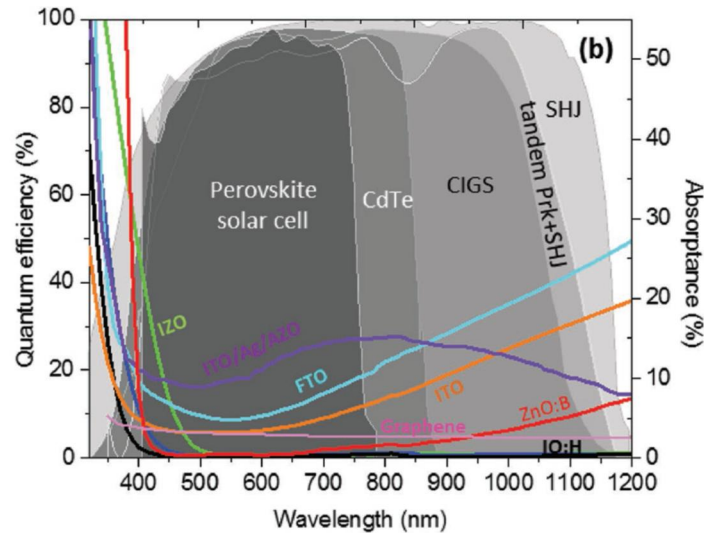


Figure 7 Quantum efficiency of various solar cells ⁷⁷⁻⁸⁰ as a function of wavelength. The absorbance curve of different transparent electrodes measured on glass substrate as a function of wavelength. ⁶⁶

Aluminum-doped ZnO (AZO) is the most widely used ZnO-based TCO ⁸¹⁻⁸⁴ which is an earth abundant polycrystal, high free carrier absorption (FCA) but lower mobility than other ZnO alloys. Chemical-bath-deposition (CBD), pulsed laser deposition (PLD), atomic layer deposition (ALD) and chemical vapor deposition (CVD) have been employed for the fabrication of these transparent electrodes ⁸⁴. Indium ZnO (IZO) is an amorphous TCO with low FCA and good optoelectronic properties, which are not much affected by post-deposition annealing, offering potential materials for temperature-sensitive applications. However, IZO has a relatively high absorption in the UV-vis range due to optical band gap narrowing ⁸³. IZO TCO has been applied in silicon heterojunction (SHJ) ⁸⁵ and perovskite solar cells ⁶³. Boron-doped ZnO (BZO) shows low NIR-IR absorbance, low free carrier densities and a particular increase of electron mobility with increasing film thickness ^{86,87}. Due to their self-texturing tendency during CVD, BZO offers excellent light-trapping for thin-film photovoltaics, which has been successfully applied in thin-film silicon ^{88,89} and CIGS ⁹⁰ solar cells.

ZnO has been used as the n-type semiconductor material in heterojunctions solar cells, such as ZnO/CdSe ⁶⁷, ZnO/CdS ⁶⁸, ZnO/Cu₂O ⁶⁹, ZnO/PbSe ⁷⁰, ZnO/Cu-Al-O ⁷¹, ZnO/ZnS and ZnO/ZnTe ⁷² heterojunctions solar cells. Although the bandgap of ZnO is too large for photovoltaic application, the quantum confinement of ZnO-based nanostructures and heterojunctions can correct the band bandgap, optical absorption and carrier localization and improve the photovoltaic performance. Metal-Organic Chemical Vapor Deposition (MOCVD) grown ZnO ^{73,74} has been recently studied as the active layer in n-ZnO/p-Si heterojunction ⁷⁵ and Schottky-junction solar cells ⁷⁶, Figure 8. These devices are attractive due to their simple structure and low cost.

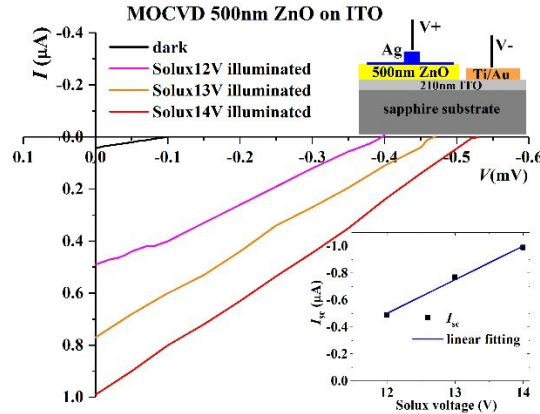


Figure 8 I-V characterization of a ZnO-based Schottky UV solar cell under various illumination intensities ⁷⁵

Dye-sensitized solar cells (DSSCs) are of great interest in the recent years, aiming at lowering the solar cell costs, as well as ensuring promising solar-energy conversion efficiency. DSSCs are based on the optical excitation of a dye, which injects an electron into the conduction band of a nanostructured wide bandgap metal oxide, and then regenerates back to its ground state by accepting one electron from a redox couple present in an electrolyte ⁶²⁻⁶⁵, Figure 9. ZnO nanostructures for DSSC has been explored extensively as the closest alternative to TiO₂ as a wide bandgap electron transport building block ^{59,62-65}.

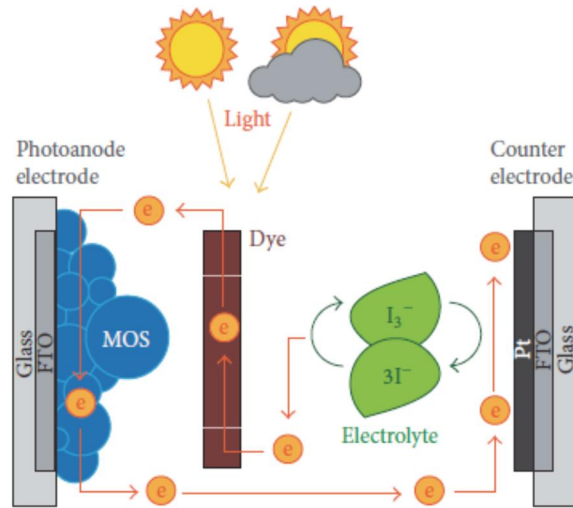


Figure 9 Schematic of a dye-sensitized solar cell. ZnO can be applied as the MOS material in the device. ⁶⁵

ZnO was the first oxide semiconductor material used as the photoanode of a DSSC ⁹¹. The highest power conversion efficiency (PCE) for ZnO-based DSSC, using liquid electrolyte, has been recorded as 7.5% ⁹¹ which is still much lower than that of a TiO₂-based DSSC (12.3%) ⁹². The solid-state ZnO-based DSSCs have much lower PCE (1-5%) compared to their counter parts with liquid electrolytes or quasi-solid state electrolytes, due to the dissolution of ZnO to Zn²⁺ by the adsorbed acidic dye, forming agglomerates (insulating layer) of Zn²⁺ and dye molecules and eventually blocking the electron injection from the dye molecules to the semiconductor ^{91,92}. To improve the ZnO-based DSSCs performance, various ZnO nanostructures are developed to improve the electron collection efficiency from the dye ^{59,62-65,93}, and the dye material are explored for to reduce Zn²⁺/dye aggregation.

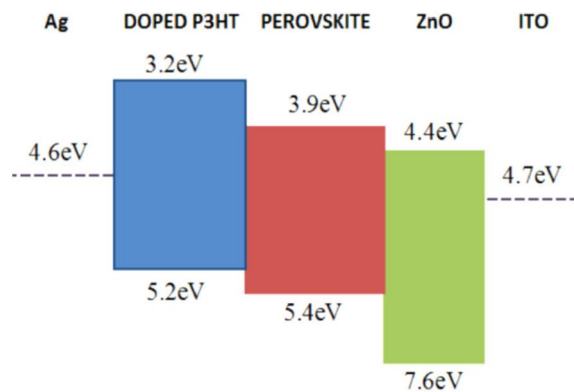


Figure 10 Schematic representation of energy band diagram of a Perovskite solar cell showing the individual HOMO and LUMO levels with work function of the electrodes. ⁹⁴

Perovskite solar cells have recently attracted much interest due to their high PCE and lower fabrication cost compared to silicon solar cells. Electron transport layer (ETL) and hole block layer (HBL) play vital roles in perovskite solar cells as electron selective contact ⁹⁵ which enhances fill factor ⁹⁶ and the open circuit voltage ⁹⁷. ZnO has a favorable conduction band energy level of 4.4 eV ⁹⁸ which extracts electrons from LUMO (Lowest Unoccupied Molecular Orbital) level (3.9 eV for methyl ammonium iodide perovskite) ⁹⁹, while the ZnO valence band energy level at 7.6 eV ⁹⁸ can efficiently block holes from HOMO (highest occupied molecular orbital level, at 5.4 eV) ⁹⁹, Figure 10. Therefore, ZnO can function as both ETL and HBL in a perovskite solar cell, making it a beneficial n-type conducting layer. In addition to the large bandgap, ZnO has a high exciton binding energy of 60 meV that contributes to an excellent chemical and thermal stability ¹⁰⁰. The highest-performing ZnO-based perovskite solar cell used a thin film ZnO nanoparticles as an ETL and achieved a PCE as high as 15.7% under AM1.5G illumination ⁹⁷.

ZnO is of great interest in photovoltaic application in recent years. Although their application in TCO and DSSCs are not as good as their counterpart TiO₂, ZnO has the advantage of non-toxicity, earth abundance, various growth techniques and nanostructure. There has been an increasing number of reports on flexible, quasi-solid state, solid state ZnO-based photovoltaic applications using various doping, nanostructures and different heterojunction materials.

4. CONCLUSIONS AND PERSPECTIVES

ZnO is a non-toxic earth abundant wide bandgap semiconductor. This material can be grown with a variety of techniques, such as sputtering, PLD, MOCVD and MBE. This paper reviews these ZnO growth techniques, and resulting crystalline quality, electrical and optical properties. There is challenge of commercializing ZnO due to native defects and difficulty in p-type doping. The main stream theories have shown that group-V elements tend to form complexes with native defects, mainly VZn. On the other hand, group-I dopants could be shallow acceptors, but the small atoms favor interstitial sites, which must be passivated before prominent p-type conductivity can be identified. A co-doping approach demonstrates more promising results in electrical properties.

ZnO-based materials offer great potential as a wide bandgap semiconductor in various applications, due to their significant structural, electrical, optical, and thermoelectric properties. This paper reviews the current state of art of ZnO in thermoelectric and photovoltaic applications. ZnO presents a large Seebeck coefficient, high thermal stability, and non-toxicity. Recent investigation on ZnO ceramics show their TE properties can be improved by various doping. ZnO also has the advantage of high electron diffusivity, high electron mobility, easy crystallization and anisotropic growth. ZnO-based nanostructures have been extensively studied as transparent electrodes, active layer, and electron transport/hole blocking layer, for dye-sensitized solar cells, hybrid organic-inorganic solar cells, and other types of solar cells.

REFERENCES

- [1] Saravanan, A., Huang, B. R., Lin, J. C., Keiser, G. and Lin, I. N., "Fast Photoresponse and Long Lifetime UV Photodetectors and Field Emitters Based on ZnO/Ultrananocrystalline Diamond Films," *Chem. - A Eur. J.* **21**(45), 16017–16026 (2015).
- [2] Tian, C., Jiang, D., Li, B., Lin, J., Zhao, Y., Yuan, W., Zhao, J., Liang, Q., Gao, S., Hou, J. and Qin, J., "Performance enhancement of ZnO UV photodetectors by surface plasmons," *ACS Appl. Mater. Interfaces* **6**(3), 2162–2166 (2014).
- [3] Kumar, R., Al-Dossary, O., Kumar, G. and Umar, A., "Zinc oxide nanostructures for no₂ gas–sensor applications: A review," *Nano-Micro Lett.* **7**(2), 1–24 (2014).
- [4] Hagedorfer, H., Lienau, K., Nishiwaki, S., Fella, C. M., Kranz, L., Uhl, A. R., Jaeger, D., Luo, L., Gretener, C., Buecheler, S., Romanyuk, Y. E. and Tiwari, A. N., "Highly transparent and conductive ZnO: Al thin films from a low temperature aqueous solution approach," *Adv. Mater.* **26**(4), 632–636 (2014).
- [5] Magnusson, E. B., Williams, B. H., Manenti, R., Nam, M. S., Nersisyan, a., Peterer, M. J., Ardavan, a. and Leek, P. J., "Surface acoustic wave devices on bulk ZnO crystals at low temperature," *Appl. Phys. Lett.* **106**(6), 4–7 (2015).
- [6] Janotti, A. and Van De Walle, C. G., "Fundamentals of zinc oxide as a semiconductor," *Reports Prog. Phys.* **72**(12) (2009).
- [7] Kim, K. H., Park, K. C. and Ma, D. Y., "Structural, electrical and optical properties of aluminum doped zinc oxide films prepared by radio frequency magnetron sputtering," *J. Appl. Phys.* **81**(12), 7764 (1997).
- [8] Minami, T., Hirotsoshi, S., Nanto, H. and Takata, S., "Group III Impurity Doped Zinc Oxide Thin Films Prepared by RF Magnetron Sputtering," *Jpn. J. Appl. Phys.* **24**(10), L871–L874 (1985).
- [9] Jin, B. J., Bae, S. H., Lee, S. Y. and Im, S., "Effects of native defects on optical and electrical properties of ZnO prepared by pulsed laser deposition," 301–305 (2000).
- [10] Shim, E. S., Kang, H. S., Kang, J. S., Kim, J. H. and Lee, S. Y., "Effect of the variation of film thickness on the structural and optical properties of ZnO thin films deposited on sapphire substrate using PLD," *Appl. Surf. Sci.* **186**(1–4), 474–476 (2002).
- [11] Kaidashev, E. M., Lorenz, M., Von Wenckstern, H., Rahm, A., Semmelhack, H. C., Han, K. H., Benndorf, G., Bundesmann, C., Hochmuth, H. and Grundmann, M., "High electron mobility of epitaxial ZnO thin films on c-plane sapphire grown by multistep pulsed-laser deposition," *Appl. Phys. Lett.* **82**(22), 3901–3903 (2003).
- [12] Yamada, A., Sang, B. and Konagai, M., "Atomic layer deposition of ZnO transparent conducting oxides," *Appl. Surf. Sci.* **112**, 216–222 (1997).
- [13] Guziewicz, E., Kowalik, I. A., Godlewski, M., Kopalko, K., Osinniy, V., Wójcik, A., Yatsunenko, S., Łusakowska, E., Paszkowicz, W. and Guziewicz, M., "Extremely low temperature growth of ZnO by atomic layer deposition," *J. Appl. Phys.* **103**(3) (2008).
- [14] Iwata, K., Fons, P., Niki, S., Yamada, A., Matsubara, K., Nakahara, K., Tanabe, T. and Takasu, H., "ZnO growth on Si by radical source MBE," *J. Cryst. Growth* **214**, 50–54 (2000).
- [15] Johnson, M. A. L., Fujita, S., Rowland, W. H., Hughes, W. C., Cook, J. W. and Schetzina, J. F., "MBE growth and properties of ZnO on sapphire and SiC substrates," *J. Electron. Mater.* **25**(5), 855–862 (1996).
- [16] Haga, K., Suzuki, T., Kashiwaba, Y., Watanabe, H., Zhang, B. P. and Segawa, Y., "High-quality ZnO films prepared on Si wafers by low-pressure MO-CVD," *Thin Solid Films* **433**(1–2 SPEC.), 131–134 (2003).
- [17] Muthukumar, S., Sheng, H., Zhong, J., Zhang, Z., Emanetoglu, N. W. and Lu, Y., "Selective MOCVD growth of ZnO nanotips," *IEEE Trans. Nanotechnol.* **2**(1), 50–54 (2003).

- [18] Kim, K. H., Park, K. C. and Ma, D. Y., “Structural, electrical and optical properties of aluminum doped zinc oxide films prepared by radio frequency magnetron sputtering,” [Http://Dx.Doi.Org/10.1063/1.365556](http://dx.doi.org/10.1063/1.365556) **7764**(1997) (1998).
- [19] McCluskey, M. D. and Jokela, S. J., “Defects in ZnO,” *J. Appl. Phys.* **106**(7) (2009).
- [20] Vidya, R., Ravindran, P., Fjellvåg, H., Svensson, B. G., Monakhov, E., Ganchenkova, M. and Nieminen, R. M., “Energetics of intrinsic defects and their complexes in ZnO investigated by density functional calculations,” *Phys. Rev. B - Condens. Matter Mater. Phys.* **83**(4), 1–12 (2011).
- [21] Park, C. H., Zhang, S. B. and Wei, S. H., “Origin of p-type doping difficulty in ZnO: The impurity perspective,” *Phys. Rev. B - Condens. Matter Mater. Phys.* **66**(7), 1–3 (2002).
- [22] Lee, E. C., Kim, Y. S., Jin, Y. G. and Chang, K. J., “Compensation mechanism for N acceptors in ZnO,” *Phys. Rev. B - Condens. Matter Mater. Phys.* **64**(8), 2–6 (2001).
- [23] Lyons, J. L., Janotti, A. and Van De Walle, C. G., “Why nitrogen cannot lead to p-type conductivity in ZnO,” *Appl. Phys. Lett.* **95**(25), 1–4 (2009).
- [24] Myers, M. A., Lee, J. H. and Wang, H., “Highly stable non-polar p-type Ag-doped ZnO thin films grown on r-cut sapphire,” *Mater. Lett.* **100**, 78–81 (2013).
- [25] Bagheri, N., Ara, M. H. M. and Ghazyani, N., “Characterization and doping effects study of high hole concentration Li-doped ZnO thin film prepared by sol-gel method,” *J. Mater. Sci. Mater. Electron.* **27**(2), 1293–1298 (2016).
- [26] Lin, S. S., “Robust low resistivity p-type ZnO:Na films after ultraviolet illumination: The elimination of grain boundaries,” *Appl. Phys. Lett.* **101**(12) (2012).
- [27] Liu, H. B., Pan, X. H., Huang, J. Y., He, H. P. and Ye, Z. Z., “Preparation of Na delta-doped p-type ZnO thin films by pulsed laser deposition using NaF and ZnO ceramic targets,” *Thin Solid Films* **540**, 53–57 (2013).
- [28] Li, Y., Pan, X. H., Jiang, J., He, H. P., Huang, J. Y., Ye, C. L. and Ye, Z. Z., “Realization of Na-doped p-type non-polar a-plane Zn_{1-x}Cd_xO films by pulsed laser deposition,” *J. Alloys Compd.* **584**, 466–470 (2014).
- [29] Tay, C. B., Chua, S. J. and Loh, K. P., “Stable p-Type Doping of ZnO Film in Aqueous Solution at Low Temperatures,” *J. Phys. Chem. C* **114**(21), 9981–9987 (2010).
- [30] Kim, Y., Lee, W., Jung, D.-R., Kim, J., Nam, S., Kim, H. and Park, B., “Optical and electronic properties of post-annealed ZnO:Al thin films,” *Appl. Phys. Lett.* **96**(17), 171902 (2010).
- [31] Kang, D. W., Kuk, S. H., Ji, K. S., Lee, H. M. and Han, M. K., “Effects of ITO precursor thickness on transparent conductive Al doped ZnO film for solar cell applications,” *Sol. Energy Mater. Sol. Cells* **95**(1), 138–141 (2011).
- [32] Mosbah, A. and Aida, M. S., “Influence of deposition temperature on structural, optical and electrical properties of sputtered Al doped ZnO thin films,” *J. Alloys Compd.* **515**, 149–153 (2012).
- [33] Cho, H. J., Lee, S. U., Hong, B., Shin, Y. D., Ju, J. Y., Kim, H. D., Park, M. and Choi, W. S., “The effect of annealing on Al-doped ZnO films deposited by RF magnetron sputtering method for transparent electrodes,” *Thin Solid Films* **518**(11), 2941–2944 (2010).
- [34] Chen, Y. J., Jen, H. W., Wong, M. S., Ho, C. H., Liang, J. H., Liu, J. T. and Pang, J. H., “The study of rapid thermal annealing on arsenic-doped ZnO for the p-type ZnO formation,” *J. Cryst. Growth* **362**(1), 193–196 (2013).
- [35] Ma, Y., Gao, Q., Wu, G. G., Li, W. C., Gao, F. B., Yin, J. Z., Zhang, B. L. and Du, G. T., “Growth and conduction mechanism of As-doped p-type ZnO thin films deposited by MOCVD,” *Mater. Res. Bull.* **48**(3), 1239–1243 (2013).

- [36] Liang, J. H., Chen, Y. J. and Wang, Y. C., "Preparation of p-type ZnO film on the GaAs substrate by thermal annealing treatment," *Surf. Coatings Technol.* **231**, 243–246 (2013).
- [37] Li, L., Shan, C. X., Li, B. H., Zhang, J. Y., Yao, B., Shen, D. Z., Fan, X. W. and Lu, Y. M., "An approach to enhanced acceptor concentration in ZnO:N films," *J. Mater. Sci.* **45**(15), 4093–4096 (2010).
- [38] Ding, M., Zhao, D., Yao, B., Li, B., Zhang, Z. and Shen, D., "The p-type ZnO film realized by a hydrothermal treatment method," *Appl. Phys. Lett.* **98**(6) (2011).
- [39] Chao, L.-C., Chen, J.-W., Peng, H.-C. and Ho, C.-H., "Characterization of nitrogen doped p-type ZnO thin films prepared by reactive ion beam sputter deposition," *Surf. Coatings Technol.* **231**, 492–495 (2013).
- [40] Snigurenko, D., Kopalko, K., Krajewski, T. A., Jakiela, R. and Guzewicz, E., "Nitrogen doped p-type ZnO films and p-n homojunction," *Semicond. Sci. Technol.* **30**(1), 15001 (2015).
- [41] Pathak, T. K., Kumar, V., Swart, H. C. and Purohit, L. P., "Effect of doping concentration on the conductivity and optical properties of p-type ZnO thin films," *Phys. B Condens. Matter* **480**, 31–35 (2016).
- [42] Chen, X., Zhang, Z., Yao, B., Zhang, Y., Gu, Y., Zhao, P., Li, B. and Shen, D., "The effect of boron on the doping efficiency of nitrogen in ZnO," *J. Alloys Compd.* **672**, 260–264 (2016).
- [43] Pathak, T. K., Kumar, V. and Purohit, L. P., "Sputtered Al-N codoped p-type transparent ZnO thin films suitable for optoelectronic devices," *Optik (Stuttg.)* **127**(2), 603–607 (2016).
- [44] Wang, Z., Zang, H. and Ren, L., "Fabrication and properties of Al-P codoped p-type zinc oxide films by RF magnetron sputtering," *Appl. Phys. A* **118**(2), 465–471 (2015).
- [45] Mohanta, S. K., Nakamura, A. and Temmyo, J., "Synthesis and characterization of N_x in co-doped MgZnO films using remote-plasma-enhanced metalorganic chemical vapor deposition," *J. Cryst. Growth* **375**, 1–5 (2013).
- [46] Li, W., Kong, C., Qin, G., Ruan, H. and Fang, L., "P-Type conductivity and stability of Ag-N codoped ZnO thin films," *J. Alloys Compd.* **609**, 173–177 (2014).
- [47] Yang, J. J., Fang, Q. Q., Wang, W. N., Wang, D. D. and Wang, C., "Pulsed laser deposition of Li-N dual acceptor in p-ZnO:(Li, N) thin film and the p-ZnO:(Li, N)/n-ZnO homojunctions on Si(100)," *J. Appl. Phys.* **115**(12), 1–6 (2014).
- [48] Sui, Y., Yao, B., Xiao, L., Xing, G., Yang, L., Li, X., Li, X., Lang, J., Lv, S., Cao, J., Gao, M. and Yang, J., "Effects of (P, N) dual acceptor doping on band gap and p-type conduction behavior of ZnO films," *J. Appl. Phys.* **113**(13) (2013).
- [49] Cao, L., Zhu, L., Jiang, J., Li, Y., Zhang, Y. and Ye, Z., "Preparation and properties of p-type Ag-doped ZnMgO thin films by pulsed laser deposition," *J. Alloys Compd.* **516**, 157–160 (2012).
- [50] Zhu, Y., Chen, M., Su, L., Su, Y., Ji, X., Gui, X. and Tang, Z., "Phase evolution, bandgap engineering and p-type conduction in undoped/N-doped BexZn1-xO alloy epitaxial films," *J. Alloys Compd.* **616**, 505–509 (2014).
- [51] Cai, H., Xu, H., Ye, Z. and Huang, J., "Realization of p-type Se-N co-doped ZnO films by radio-frequency magnetron sputtering," *Mater. Lett.* **108**, 183–185 (2013).
- [52] Tang, K., Gu, S., Wu, K., Zhu, S., Ye, J., Zhang, R. and Zheng, Y., "Tellurium assisted realization of p-type N-doped ZnO," *Appl. Phys. Lett.* **96**(24) (2010).
- [53] Tang, K., Gu, S., Ye, J., Zhu, S., Huang, S., Gu, R., Zhang, R., Shi, Y. and Zheng, Y., "Mutually beneficial doping of tellurium and nitrogen in ZnO films grown by metal-organic chemical vapor deposition," *J. Vac. Sci. Technol. A Vacuum, Surfaces, Film.* **30**(5), 51508 (2012).
- [54] Park, S., Minegishi, T., Oh, D., Lee, H., Taishi, T., Park, J., Jung, M., Chang, J., Im, I., Ha, J., Hong, S., Yonenaga, I., Chikyow, T. and Yao, T., "High-quality p-type ZnO films grown by Co-doping of N and Te on Zn-face ZnO substrates," *Appl. Phys. Express* **3**(3) (2010).

- [55] Kang, J.-W., Choi, Y.-S., Kim, B.-H., Kim, N.-Y., Tu, C. W. and Park, S.-J., "Structural and electrical properties of phosphorous-doped p-type ZnSxO1-x film grown by co-sputtering," *Scr. Mater.* **84–85**, 39–42 (2014).
- [56] Colder, H., Guilmeau, E., Harnois, C., Marinel, S., Retoux, R. and Savary, E., "Preparation of Ni-doped ZnO ceramics for thermoelectric applications," *J. Eur. Ceram. Soc.* **31**(15), 2957–2963 (2011).
- [57] Jung, K., Lee, K. H., Seo, W. and Choi, S., "An enhancement of a thermoelectric power factor in a Ga-doped ZnO system : A chemical compression by enlarged Ga solubility An enhancement of a thermoelectric power factor in a Ga-doped ZnO system : A chemical compression by enlarged Ga solubility," 1–5 (2012).
- [58] Fan, P., Zheng, Z. H., Li, Y. Z., Lin, Q. Y., Luo, J. T., Liang, G. X., Cai, X. M., Zhang, D. P. and Ye, F., "Low-cost flexible thin film thermoelectric generator on zinc based thermoelectric materials," *Appl. Phys. Lett.* **106**(7), 0–4 (2015).
- [59] Djurišić, A. B., Chen, X., Leung, Y. H. and Man Ching Ng, A., "ZnO nanostructures: growth, properties and applications," *J. Mater. Chem.* **22**(14), 6526 (2012).
- [60] Huang, J., Yin, Z. and Zheng, Q., "Applications of ZnO in organic and hybrid solar cells," *Energy Environ. Sci.* **4**(10), 3861 (2011).
- [61] Fortunato, E., Ginley, D., Hosono, H. and Paine, D. C., "Transparent Conducting Oxides for Photovoltaics," *MRS Bull.* **32**(3), 242–247 (2007).
- [62] Vittal, R. and Ho, K. C., "Zinc oxide based dye-sensitized solar cells: A review," *Renew. Sustain. Energy Rev.* **70**(December 2016), 920–935 (2017).
- [63] Zhang, Q., Dandeneau, C. S., Zhou, X. and Cao, G., "ZnO Nanostructures for Dye-Sensitized Solar Cells," *Adv. Mater.* **21**(41), 4087–4108 (2009).
- [64] Kumar, R., Umar, A., Kumar, G., Nalwa, H. S., Kumar, A. and Akhtar, M. S., "Zinc oxide nanostructure-based dye-sensitized solar cells," *J. Mater. Sci.* **52**(9), 4743–4795 (2017).
- [65] Cavallo, C., Di Pascasio, F., Latini, A., Bonomo, M. and Dini, D., "Nanostructured Semiconductor Materials for Dye-Sensitized Solar Cells," *J. Nanomater.* **2017** (2017).
- [66] Morales-Masis, M., De Wolf, S., Woods-Robinson, R., Ager, J. W. and Ballif, C., "Transparent Electrodes for Efficient Optoelectronics," *Adv. Electron. Mater.* **3**(5) (2017).
- [67] Lévy-Clément, C., Tena-Zaera, R., Ryan, M. A., Katty, A. and Hodes, G., "CdSe-sensitized p-CuSCN/nanowire n-ZnO heterojunctions," *Adv. Mater.* **17**(12), 1512–1515 (2005).
- [68] Kundu, P., Deshpande, P. A., Madras, G. and Ravishankar, N., "Nanoscale ZnO/CdS heterostructures with engineered interfaces for high photocatalytic activity under solar radiation," *J. Mater. Chem.* **21**(12), 4209 (2011).
- [69] Nishi, Y., Miyata, T. and Minami, T., "The impact of heterojunction formation temperature on obtainable conversion efficiency in n-ZnO/p-Cu₂O solar cells," *Thin Solid Films* **528**, 72–76 (2013).
- [70] Leschkies, K. S., Beatty, T. J., Kang, M. S., Norris, D. J. and Aydil, E. S., "Solar cells based on junctions between colloidal Pbse nanocrystals and thin ZnO films," *ACS Nano* **3**(11), 3638–3648 (2009).
- [71] Tonooka, K., Bando, H. and Aiura, Y., "Photovoltaic effect observed in transparent p-n heterojunctions based on oxide semiconductors," *Thin Solid Films* **445**(2), 327–331 (2003).
- [72] Schrier, J., Demchenko, D. O., Alivisatos, A. P., Science, M., Di, V. and Berkeley, L., "Optical Properties of ZnO / ZnS and ZnO / ZnTe Heterostructures for Photovoltaic Applications" (2007).
- [73] Pan, M., Nause, J., Rengarajan, V., Rondon, R., Park, E. H. and Ferguson, I. T., "Epitaxial growth and characterization of p-type ZnO," *J. Electron. Mater.* **36**(4), 457–461 (2007).

- [74] Pan, M., Fenwick, W. E., Strassburg, M., Li, N., Kang, H., Kane, M. H., Asghar, A., Gupta, S., Varatharajan, R., Nause, J., El-Zein, N., Fabiano, P., Steiner, T. and Ferguson, I., “Metal-organic chemical vapor deposition of ZnO,” *J. Cryst. Growth* **287**(2), 688–693 (2006).
- [75] Zhou, C., Ghods, A., Yunghans, K. L., Saravade, V. G., Patel, P. V., Jiang, X., Kucukgok, B., Lu, N. and Ferguson, I., “ZnO for solar cell and thermoelectric applications,” 101051K (2017).
- [76] Hussain, B., Ebong, A. and Ferguson, I., “Zinc Oxide and Silicon Based Heterojunction Solar Cell Model,” 8–11 (2015).
- [77] Wright, M. and Uddin, A., “Organic-inorganic hybrid solar cells: A comparative review,” *Sol. Energy Mater. Sol. Cells* **107**, 87–111 (2012).
- [78] Klein, A., Körber, C., Wachau, A., Säuberlich, F., Gassenbauer, Y., Harvey, S. P., Proffit, D. E. and Mason, T. O., “Transparent conducting oxides for photovoltaics: Manipulation of fermi level, work function and energy band alignment,” *Materials (Basel)*. **3**(11), 4892–4914 (2010).
- [79] Saliba, M., Matsui, T., Seo, J.-Y., Domanski, K., Correa-Baena, J.-P., Nazeeruddin, M. K., Zakeeruddin, S. M., Tress, W., Abate, A., Hagfeldt, A. and Grätzel, M., “Cesium-containing triple cation perovskite solar cells: improved stability, reproducibility and high efficiency,” *Energy Environ. Sci.* **9**(6), 1989–1997 (2016).
- [80] Werner, J., Barraud, L., Walter, A., Bräuninger, M., Sahli, F., Sacchetto, D., Tétreault, N., Paviet-Salomon, B., Moon, S. J., Allebé, C., Despeisse, M., Nicolay, S., De Wolf, S., Niesen, B. and Ballif, C., “Efficient Near-Infrared-Transparent Perovskite Solar Cells Enabling Direct Comparison of 4-Terminal and Monolithic Perovskite/Silicon Tandem Cells,” *ACS Energy Lett.* **1**(2), 474–480 (2016).
- [81] Holman, Z. C., Descoedres, a, De Wolf, S. and Ballif, C., “Record Infrared Internal Quantum Efficiency in Silicon Heterojunction Solar Cells With Dielectric/Metal Rear Reflectors,” *IEEE J. Photovoltaics* **3**(4), 1243–1249 (2013).
- [82] Barnes, T. M., Reese, M. O., Bergeson, J. D., Larsen, B. A., Blackburn, J. L., Beard, M. C., Bult, J. and Van De Lagemaat, J., “Comparing the fundamental physics and device performance of transparent, conductive nanostructured networks with conventional transparent conducting oxides,” *Adv. Energy Mater.* **2**(3), 353–360 (2012).
- [83] Berginski, M., Hüpkes, J., Schulte, M., Schöpe, G., Stiebig, H., Rech, B. and Wuttig, M., “The effect of front ZnO:Al surface texture and optical transparency on efficient light trapping in silicon thin-film solar cells,” *J. Appl. Phys.* **101**(7) (2007).
- [84] Dabirian, A., Martin De Nicolas, S., Niesen, B., Hessler-Wyser, A., De Wolf, S., Morales-Masis, M. and Ballif, C., “Tuning the Optoelectronic Properties of ZnO:Al by Addition of Silica for Light Trapping in High-Efficiency Crystalline Si Solar Cells,” *Adv. Mater. Interfaces* **3**(3) (2016).
- [85] Gordon, R. G., “C riteria for Choosing Transparent Conductors,” *History*(August), 52–57 (2000).
- [86] Morales-Masis, M., Martin De Nicolas, S., Holovsky, J., De Wolf, S. and Ballif, C., “Low-Temperature High-Mobility Amorphous IZO for Silicon Heterojunction Solar Cells,” *IEEE J. Photovoltaics* **5**(5), 1340–1347 (2015).
- [87] Werner, J., Dubuis, G., Walter, A., Löper, P., Moon, S. J., Nicolay, S., Morales-Masis, M., De Wolf, S., Niesen, B. and Ballif, C., “Sputtered rear electrode with broadband transparency for perovskite solar cells,” *Sol. Energy Mater. Sol. Cells* **141**, 407–413 (2015).
- [88] Fanni, L., Aebersold, A. B., Morales-Masis, M., Alexander, D. T. L., Hessler-Wyser, A., Nicolay, S., H??bert, C. and Ballif, C., “Increasing Polycrystalline Zinc Oxide Grain Size by Control of Film Preferential Orientation,” *Cryst. Growth Des.* **15**(12), 5886–5891 (2015).
- [89] Fay, S., Feitknecht, L., Schlüchter, R., Kroll, U., Vallat-Sauvain, E. and Shah, A., “Rough ZnO layers by LP-CVD process and their effect in improving performances of amorphous and microcrystalline silicon solar cells,”

Sol. Energy Mater. Sol. Cells **90**(18–19), 2960–2967 (2006).

- [90] Ding, L., Fanni, L., Messerschmidt, D., Zabihzadeh, S., Masis, M. M., Nicolay, S. and Ballif, C., “Tailoring the surface morphology of zinc oxide films for high-performance micromorph solar cells,” Sol. Energy Mater. Sol. Cells **128**, 378–385 (2014).
- [91] Memarian, N., Concina, I., Braga, A., Rozati, S. M., Vomiero, A. and Sberveglieri, G., “Hierarchically assembled ZnO nanocrystallites for high-efficiency dye-sensitized solar cells,” Angew. Chemie - Int. Ed. **50**(51), 12321–12325 (2011).
- [92] A. Yella, H-W. Lee, H.N. Tsao, C. Yi, A.K. Chandiran, M. N., “Porphyrin-sensitized solar cells with cobalt (II/III)-based redox electrolyte exceed 12 percent efficiency,” Science (80-.). **334**(6056), 629 (2011).
- [93] Law, M., Greene, L. E., Radenovic, A., Kuykendall, T., Liphardt, J. and Yang, P., “ZnO-Al₂O₃ and ZnO-TiO₂ core-shell nanowire dye-sensitized solar cells,” J. Phys. Chem. B **110**(45), 22652–22663 (2006).
- [94] Mahmud, M. A., Elumalai, N. K., Upama, M. B., Wang, D., Chan, K. H., Wright, M., Xu, C., Haque, F. and Uddin, A., “Low temperature processed ZnO thin film as electron transport layer for efficient perovskite solar cells,” Sol. Energy Mater. Sol. Cells **159**, 251–264 (2017).
- [95] Hu, Q., Wu, J., Jiang, C., Liu, T., Que, X., Zhu, R. and Gong, Q., “Engineering of electron-selective contact for perovskite solar cells with efficiency exceeding 15%,” ACS Nano **8**(10), 10161–10167 (2014).
- [96] Juarez-Perez, E. J., Wußler, M., Fabregat-Santiago, F., Lakus-Wollny, K., Mankel, E., Mayer, T., Jaegermann, W. and Mora-Sero, I., “Role of the selective contacts in the performance of lead halide perovskite solar cells,” J. Phys. Chem. Lett. **5**(4), 680–685 (2014).
- [97] Liu, D. and Kelly, T. L., “Perovskite solar cells with a planar heterojunction structure prepared using room-temperature solution processing techniques,” Nat. Photonics **8**(2), 133–138 (2014).
- [98] Choi, H., Mai, C.-K., Kim, H.-B., Jeong, J., Song, S., Bazan, G. C., Kim, J. Y. and Heeger, A. J., “Conjugated polyelectrolyte hole transport layer for inverted-type perovskite solar cells,” Nat. Commun. **6**, 7348 (2015).
- [99] Gu, Y., Lu, H., Geng, Y., Ye, Z., Zhang, Y., Sun, Q., Ding, S. and Zhang, D. W., “Optical and microstructural properties of ZnO/TiO₂ nanolaminates prepared by atomic layer deposition,” Nanoscale Res. Lett. **8**(1), 107 (2013).
- [100] Son, D. Y., Bae, K. H., Kim, H. S. and Park, N. G., “Effects of seed layer on growth of ZnO nanorod and performance of perovskite solar cell,” J. Phys. Chem. C **119**(19), 10321–10328 (2015).